

# Quantum correlations in critical $XXZ$ system and LMG model

Biao-Liang Ye,<sup>1</sup> Bo Li,<sup>2,3</sup> Xianqing Li-Jost,<sup>3</sup> and Shao-Ming Fei<sup>3,4</sup>

<sup>1</sup>*School of Physics and Electronic Information, Shangrao Normal University, Shangrao 334001, China*

<sup>2</sup>*School of Mathematics and Computer Sciences, Shangrao Normal University, Shangrao 334001, China*

<sup>3</sup>*Max-Planck-Institute for Mathematics in the Sciences, Leipzig 04103, Germany*

<sup>4</sup>*School of Mathematical Sciences, Capital Normal University, Beijing 100048, China*

(Dated: October 3, 2018)

We investigate the quantum phase transitions for the  $XXZ$  spin-1/2 chains via the quantum correlations between the nearest and next to nearest neighbor spins characterized by negativity, information deficit, trace distance discord and local quantum uncertainty. It is shown that all these correlations exhibit the quantum phase transitions at  $\Delta = -1$ . However, only information deficit and local quantum uncertainty can demonstrate quantum phase transitions at  $\Delta = 1$ . The analytical and numerical behaviors of the quantum correlations for the  $XXZ$  system are presented. We also consider quantum correlations in the Hartree-Fock ground state of the Lipkin-Meshkov-Glick (LMG) model.

PACS numbers: 03.67.-a, 64.70.Tg, 75.10.Pq

## I. INTRODUCTION

Quantum entanglement is an ubiquitous resource in quantum information processing [1] and has many significant applications in quantum information tasks [2]. Besides quantum entanglement, there are also quantum correlations that can be used to realize some quantum speed up without entanglement [3]. Much attentions have been paid to all such nonclassical correlations [4]. Many measures to quantify nonclassical correlations have been proposed [5], including quantum discord [6] and information deficit [7]. A geometric method in quantifying quantum discord has been provided in [8]. The analytical expressions of quantum correlation for arbitrary two-qubit  $X$  states have been presented via trace distance discord [9]. Inspired by Wigner-Yanase Skew information, in Ref.[10] the local quantum uncertainty is proposed to quantify nonclassical correlations.

On the other hand, quantum phase transition is a fundamental phenomena in condensed matter physics, and is tightly related to quantum correlations. In Ref. [11, 12], the authors utilize the entanglement of formation and quantum discord to spotlight the quantum critical points for the  $XXZ$  model,  $XY$  model, and the Ising model with external magnetic field at finite temperatures. In Ref. [13] the authors used quantum discord and classical correlation to detect quantum phase transitions for  $XY$  spin chain with three-spin interactions at both zero and finite temperatures. The authors in [14] revealed a general quantum phase transition in an infinite one-dimensional  $XXZ$  chain in terms of concurrence and Bell inequalities. In terms of the density matrix renormalization group theory method, the behaviors of the quantum discord, quantum coherence and Wigner-Yansase skew information the relations between the phase transitions and symmetry points in the Heisenberg  $XXZ$  spin-1 chains have been extensively investigated in [15]. The classical correlation and quantum discord also exhibit the signatures of the quantum phase transitions of  $XXZ$

model and the Lipkin-Meshkov-Glick (LMG) model [16].

Although the Heisenberg  $XXZ$  model has been extensively investigated from different perspectives owing to its rich physics, the quantum correlations used in studying quantum phase transitions concern almost only concurrence and quantum discord. It would be interesting if other quantum correlations can also reveal general quantum phase transitions. In this work, we take negativity, information deficit, trace distance discord, and local quantum uncertainty to study the quantum phase transitions of the  $XXZ$  spin-1/2 chains, as well as the quantum correlations in the Hartree-Fock ground state of the Lipkin-Meshkov-Glick model. In sect. II, we review several basic notations and concepts of measures of quantum correlations. In sect. III, the Heisenberg  $XXZ$  model is introduced. We discuss the computation of the quantum correlations and illustrate the results for the  $XXZ$  chain. In sect. IV, analytical and numerical results for all the quantum correlations are demonstrated for the LMG model. Finally, we conclude in sect. V.

## II. MEASURES OF QUANTUM CORRELATIONS

Let us first review the basic notations and concepts of several quantum correlation measures.

**Negativity** Negativity is a computable measure of quantum entanglement [17]. It can be calculated effectively for any mixed states of arbitrary bipartite systems. The negativity  $\mathcal{N}(\rho_{AB})$  of a bipartite state  $\rho_{AB}$  is defined by

$$\mathcal{N} = \frac{\|\rho^{TA}\|_1 - 1}{2} = \left| \sum_i \mu_i \right|, \quad (1)$$

where  $\rho^{TA}$  is the partially transposed state of  $\rho_{AB}$  with respect to the subsystem  $A$ ,  $\|\sigma\|_1 = \text{Tr}\sqrt{\sigma^\dagger\sigma}$  denotes the trace norm one (or Schatten one-norm) of an Hermitian

operator  $\sigma$ , and  $\mu_i$  are the negative eigenvalues of  $\varrho^{TA}$  show how much  $\varrho^{TA}$  fails to be positive definite.

**Information deficit** Let  $\Pi_j^A$  denote a local complete projective measurement on subsystem  $A$ , which satisfy  $\sum_j \Pi_j^A = I_A$  and  $\Pi_j^A \Pi_k^A = \delta_{jk} \Pi_k^A$ , with  $I_A$  being the identity operator on subsystem  $A$ . For the case that  $\varrho_A = \text{Tr}_B(\varrho_{AB})$  is a single-qubit state, the rank-1 projectors are of the form  $\Pi_j^A = |\Omega_j\rangle\langle\Omega_j|$ ,  $j = 0, 1$ , where

$$\begin{aligned} |\Omega_0\rangle &= \cos\theta|0\rangle + e^{i\varphi}\sin\theta|1\rangle, \\ |\Omega_1\rangle &= -e^{-i\varphi}\sin\theta|0\rangle + \cos\theta|1\rangle, \end{aligned} \quad (2)$$

with  $0 \leq \theta \leq \pi$ ,  $0 \leq \varphi < 2\pi$ , and  $\{|0\rangle, |1\rangle\}$  the computational basis of the subsystem  $A$ .

After the projective measurement, the state  $\varrho_{AB}$  of the total system becomes

$$\varrho'_{AB} = \sum_j \Pi_j^A \varrho_{AB} \Pi_j^A. \quad (3)$$

The information deficit is the minimum information loss by the measurement,

$$\mathcal{I}(\varrho_{AB}) = \min_{\Pi_j^A} S(\varrho'_{AB}) - S(\varrho_{AB}), \quad (4)$$

where  $S(\varrho) = -\text{Tr}\varrho \log \varrho$  is the von Neumann entropy and  $\log$  is in base 2. Here we use the definition of information deficit instead of the one-way information deficit [7, 18, 19] for brevity. Similar to the quantum discord [6], the analytical expressions for the information deficit of the simplest two-qubit states are still not known yet [20].

**Trace distance discord** The definition of trace distance discord is given by

$$\mathcal{D}(\varrho_{AB}) = \frac{1}{2} \min_{\Pi_j^A} \|\varrho_{AB} - \varrho'_{AB}\|_1. \quad (5)$$

Here, the trace norm one  $\|\cdot\|_1$  is the same as the one in Eq.(1), and the  $\varrho'_{AB}$  is the state after measurement on subsystem  $A$  in Eq.(3).

Trace distance discord is a reliable geometric quantifier of discord-like correlations [9]. It provides an explicit and compact expression for two-qubit  $X$  states.

**Local quantum uncertainty** Uncertainty of local observables for a bipartite system is a *bona fide* measure of nonclassical correlation. Local quantum uncertainty can play important roles in the context of quantum metrology.

Local quantum uncertainty is the minimum skew information [21, 22] achievable by local measurements. The minimum achievable skew information by a single local measurement is given by

$$\mathcal{U} = \min_{K^\Gamma} I(\varrho, K^\Gamma), \quad (6)$$

where  $\Gamma$  denotes the spectrum of  $K^\Gamma$ , and the minimization over a chosen spectrum of observables leads

to a specific measure from the family and  $I(\varrho, K^\Gamma) = -\frac{1}{2} \text{Tr}([\sqrt{\varrho}, K^\Gamma]^2)$ . However, for a two-qubit system, all of the members of the family turn out to be equivalent. For two-qubit system, the local quantum uncertainty admits a closed formula. The local quantum uncertainty with respect to subsystem  $A$  can be derived by

$$\mathcal{U} = 1 - \lambda_{\max}\{W_{AB}\}, \quad (7)$$

where  $\lambda_{\max}$  is the maximum eigenvalues and  $W_{AB}$  denotes a  $3 \times 3$  symmetric matrix whose elements are given by

$$(W_{AB})_{uv} = \text{Tr}\{\varrho_{AB}^{1/2}(\sigma_A^u \otimes I_B)\varrho_{AB}^{1/2}(\sigma_A^v \otimes I_B)\}, \quad (8)$$

with  $\sigma_A^{u(v)}$  being the Pauli matrices,  $u, v = x, y, z$ .

### III. HEISENBERG $XXZ$ SPIN-1/2 CHAIN

We now consider the one-dimensional spin chain with anisotropic Heisenberg interactions. The Hamiltonian of the  $XXZ$  model is given by

$$H = \sum_{j=1}^N [S_j^x S_{j+1}^x + S_j^y S_{j+1}^y + \Delta S_j^z S_{j+1}^z], \quad (9)$$

where  $S_j^u = \sigma_j^u/2$  ( $u = x, y, z$ ),  $\sigma_j^u$  are the Pauli operators on site  $j$ ,  $\Delta$  is the anisotropic parameter,  $\sigma_{j+N}^u = \sigma_j^u$ , and  $N$  is the number of spins of the chain. For  $T = 0$  the  $XXZ$  model has two critical points [23]. The first-order transition happens at  $\Delta = -1$  and a continuous phase transition shows up at  $\Delta = 1$ .

Due to symmetry in the spin chain model with Hamiltonian Eq.(9), the two-qubit reduced density matrix of sites  $i$  and  $i+r$  in the basis  $|1\rangle = |\uparrow\uparrow\rangle$ ,  $|2\rangle = |\uparrow\downarrow\rangle$ ,  $|3\rangle = |\downarrow\uparrow\rangle$ ,  $|4\rangle = |\downarrow\downarrow\rangle$  (where  $|\uparrow\rangle$  and  $|\downarrow\rangle$  are the eigenstates of the Pauli spin  $z$ -operator) has the following form,

$$\varrho_{AB} = \begin{pmatrix} \varrho_{11} & 0 & 0 & 0 \\ 0 & \varrho_{22} & \varrho_{23} & 0 \\ 0 & \varrho_{32} & \varrho_{33} & 0 \\ 0 & 0 & 0 & \varrho_{44} \end{pmatrix}, \quad (10)$$

with

$$\varrho_{23} = \varrho_{32} = \frac{\langle \sigma_i^x \sigma_{i+r}^x \rangle}{2},$$

$$\varrho_{11} = \varrho_{44} = \frac{1 + \langle \sigma_i^z \sigma_{i+r}^z \rangle}{4},$$

and

$$\varrho_{22} = \varrho_{33} = \frac{1 - \langle \sigma_i^z \sigma_{i+r}^z \rangle}{4}.$$

The correlation functions for nearest neighbor ( $r=1$ ) spins of  $XXZ$  model. The two point correlation functions of the  $XXZ$  model at zero temperature and in the

thermodynamics limit can be derived by using the Bethe ansatz technique [24]. The spin-spin correlation functions

$$\langle \sigma_i^z \sigma_{i+1}^z \rangle = 1 + 2 \int_{-\infty+i/2}^{\infty+i/2} \frac{dx}{\sinh(\pi x)} \left( \cot(\nu x) \coth(\nu) - \frac{x}{\sin^2(\nu x)} \right), \quad (11)$$

and

$$\langle \sigma_i^x \sigma_{i+1}^x \rangle = \int_{-\infty+i/2}^{\infty+i/2} \frac{dx}{\sinh(\pi x)} \left( \frac{x}{\sin^2(\nu x)} \cosh \nu - \frac{\cot(\nu x)}{\sinh \nu} \right), \quad (12)$$

with  $\nu = \cosh^{-1} \Delta$ . For  $\Delta = 1$ ,  $\langle \sigma_i^x \sigma_{i+1}^x \rangle = \langle \sigma_i^z \sigma_{i+1}^z \rangle = 1/3(1 - 4 \ln 2)$ , and for  $\Delta \leq -1$ ,  $\langle \sigma_i^z \sigma_{i+1}^z \rangle = 1$  and

between nearest-neighbor spin sites for  $\Delta > 1$  are given by Takahashi et al. [25]

$\langle \sigma_i^x \sigma_{i+1}^x \rangle = 0$  [14].

For  $-1 < \Delta < 1$ , the correlation functions are given by Kato et al. [26]

$$\langle \sigma_i^z \sigma_{i+1}^z \rangle = 1 - \frac{2}{\pi^2} \int_{-\infty}^{\infty} \frac{dx}{\sinh x} \frac{x \cosh x}{\cosh^2(\Phi x)} + \frac{2 \cot(\pi \Phi)}{\pi} \int_{-\infty}^{\infty} \frac{dx}{\sinh x} \frac{\sinh((1 - \Phi)x)}{\cosh(\Phi x)}, \quad (13)$$

and

$$\langle \sigma_i^x \sigma_{i+1}^x \rangle = \frac{\cos(\pi \Phi)}{\pi^2} \int_{-\infty}^{\infty} \frac{dx}{\sinh x} \frac{x \cosh x}{\cosh^2(\Phi x)} - \frac{1}{\pi \sin(\pi \Phi)} \int_{-\infty}^{\infty} \frac{dx}{\sinh x} \frac{\sinh((1 - \Phi)x)}{\cosh(\Phi x)}, \quad (14)$$

with  $\Phi = \frac{1}{\pi} \cos^{-1} \Delta$ .

*The correlation functions for next to nearest neighbor*

( $r=2$ ) spins of  $XXZ$  model. For the next to nearest-neighbor spins, in the region  $\Delta > 1$ , we have the correlation functions [25],

$$\langle \sigma_i^x \sigma_{i+2}^x \rangle = \int_{-\infty+i/2}^{\infty+i/2} \frac{dx}{\sinh(\pi x)} \frac{1}{2} \left[ -\frac{x}{\sin^2(\nu x)} \left( \frac{3 \sinh^2 \nu}{\sin^2(\nu x)} + 1 - 3 \cosh 2\nu \right) + \cot(\nu x) \left( \frac{3 \cosh(2\nu) \tanh(\nu)}{\sin^2(\nu x)} - \frac{4}{\sinh(2\nu)} \right) \right],$$

and

$$\langle \sigma_i^z \sigma_{i+2}^z \rangle = 1 + \int_{-\infty+i/2}^{\infty+i/2} \frac{dx}{\sinh(\pi x)} \left[ \frac{x}{\sin^2(\nu x)} \left( \frac{3 \sinh^2 \nu}{\sin^2(\nu x)} - 1 - \cosh(2\nu) \right) - \cot(\nu x) \left( \frac{3 \tanh \nu}{\sin^2(\nu x)} - 4 \coth(2\nu) \right) \right]. \quad (15)$$

with  $\nu = \cosh^{-1} \Delta$ . For  $\Delta \leq -1$ ,  $\langle \sigma_i^z \sigma_{i+1}^z \rangle = 1$  and

$\langle \sigma_i^x \sigma_{i+1}^x \rangle = 0$ . If  $\Delta = 1$  [24], then  $\langle \sigma_i^x \sigma_{i+2}^x \rangle = \langle \sigma_i^z \sigma_{i+2}^z \rangle = 0.242719$ . For  $-1 < \Delta < 1$  one has [27]

$$\begin{aligned} \langle \sigma_i^x \sigma_{i+2}^x \rangle = & - \int_{-\infty}^{\infty} \frac{dx}{\sinh x} \frac{\sinh(1 - \Phi)x}{\cosh(\Phi x)} \left[ \frac{2}{\pi \sin(2\pi \Phi)} + \frac{3 \cos 2\pi \Phi \tan \pi \Phi}{\pi^3} x^2 \right] \\ & + \int_{-\infty}^{\infty} \frac{dx}{\sinh x} \frac{\cosh x}{(\cosh \Phi x)^2} \left[ \frac{\cos 2\pi \Phi}{\pi^2} x + \frac{(\sin \pi \Phi)^2}{\pi^4} x^3 \right] \end{aligned} \quad (16)$$

and

$$\begin{aligned} \langle \sigma_i^z \sigma_{i+2}^z \rangle = & 1 + 4 \int_{-\infty}^{\infty} \frac{dx}{\sinh x} \frac{\sinh(1 - \Phi)x}{\cosh \Phi x} \left[ \frac{\cot(2\pi \Phi)}{\pi} + \frac{3 \tan \pi \Phi}{2\pi^3} x^2 \right] \\ & - 4 \int_{-\infty}^{\infty} \frac{dx}{\sinh x} \frac{\cosh x}{(\cosh \Phi x)^2} \left[ \frac{x}{2\pi^2} + \frac{(\sin \pi \Phi)^2}{2\pi^4} x^3 \right]. \end{aligned} \quad (17)$$

i) By the definition of *negativity* Eq.(1), we have for the nearest neighbor spins of  $XXZ$  model,

$$\mathcal{N} = -\frac{1}{4}(1 + \langle \sigma_i^z \sigma_{i+1}^z \rangle + 2\langle \sigma_i^x \sigma_{i+1}^x \rangle). \quad (18)$$

For the next to nearest neighbor spins, the analytical formula of negativity about the  $XXZ$  model is given by

$$\mathcal{N} = -\frac{1}{4}(1 + \langle \sigma_i^z \sigma_{i+2}^z \rangle - 2\langle \sigma_i^x \sigma_{i+2}^x \rangle), \quad (19)$$

in region  $\Delta \in (-1, -0.358733)$ , and  $\mathcal{N} = 0$  for others region of  $\Delta$ , see Fig. (1) for the behaviors of quantum entanglement  $\mathcal{N}$ .

From Fig. (1), we observe that, for the nearest neighbor spins, the negativity increases monotonously with

anisotropy in the region  $-1 < \Delta < 1$ , while in the region  $\Delta > 1$  the negativity decreases as anisotropy increases. And the entanglement reaches the maximal value at  $\Delta = 1$ . For the next to nearest neighbor spins, only in the region  $\Delta \in (-1, -0.358733)$  the entanglement is non-zero. Moreover, the sudden birth of entanglement happens at  $\Delta = -1$  both for the nearest and next to nearest neighbor spins. From the right figure one can see that the transition happens also at the critical point  $\Delta = -1$ .

ii) We take the *information deficit* to capture the quantum correlation of the  $XXZ$  system. In the parameter region  $-1 < \Delta < 1$ , the optimal projective measurement bases (2) are obtained at  $\theta = \pi/4$  and  $\varphi = 0$ . We have the analytical expression of information deficit for the nearest neighbor spins,

$$\begin{aligned} \mathcal{I} = & \frac{1}{4} \{ 2(1 + \langle \sigma_i^z \sigma_{i+1}^z \rangle) \log(1 + \langle \sigma_i^z \sigma_{i+1}^z \rangle) - \sum_{\pm} [2(1 \pm \langle \sigma_i^x \sigma_{i+1}^x \rangle) \log(1 \pm \langle \sigma_i^x \sigma_{i+1}^x \rangle) \\ & - (1 - \langle \sigma_i^z \sigma_{i+1}^z \rangle \pm 2\langle \sigma_i^x \sigma_{i+1}^x \rangle) \log(1 - \langle \sigma_i^z \sigma_{i+1}^z \rangle \pm 2\langle \sigma_i^x \sigma_{i+1}^x \rangle)] \}. \end{aligned} \quad (20)$$

For other regions of  $\Delta$ , the optimal measurement are given by  $\theta = 0$  and  $\varphi = 0$ . We have

$$\begin{aligned} \mathcal{I} = & \frac{1}{4} \{ \sum_{\pm} [(1 - \langle \sigma_i^z \sigma_{i+1}^z \rangle \pm 2\langle \sigma_i^x \sigma_{i+1}^x \rangle) \log(1 - \langle \sigma_i^z \sigma_{i+1}^z \rangle \pm 2\langle \sigma_i^x \sigma_{i+1}^x \rangle) \\ & - 2(1 - \langle \sigma_i^z \sigma_{i+1}^z \rangle) \log(1 - \langle \sigma_i^z \sigma_{i+1}^z \rangle)] \}. \end{aligned} \quad (21)$$

The analytical expression of information deficit for the next to nearest neighbor spins is in coincidence with the nearest neighbor spins. However, their scales are different (see Fig.2). In fact, the above exact expressions of information deficit are also adapted for quantum discord [28].

From Fig.(2), we see that the information deficit in the region  $\Delta > 1$  decreases monotonously with anisotropy  $\Delta$  for both the nearest and next to nearest neighbor spins. There are two critical points at  $\Delta = -1$  and 1 in the derivative of information deficit with respect to  $\Delta$ , showing a kind of quantum phase transitions for the  $XXZ$  spin-1/2 chain.

iii) *Trace distance discord*. For the nearest neighbor

spins, the analytical expression of trace distance discord is given by  $\mathcal{D} = |\langle \sigma_i^x \sigma_{i+1}^x \rangle|/2$ , which is also the formula for the next to nearest neighbor spins.

For the nearest neighbor spins, the trace distance discord increases monotonously with anisotropy in the region  $-1 < \Delta < 0$ , while in the region  $\Delta \geq 0$ , it decreases as anisotropy  $\Delta$  increases (see Fig. (3)). A sudden change happens at  $\Delta = -1$  both for the nearest and next to nearest neighbor spins, giving rise to quantum phase transitions of the  $XXZ$  model.

iv) The analytical formula of the *local quantum uncertainty* for both nearest and next to nearest neighbor spins can be written as

$$\mathcal{U} = 1 - \begin{cases} \sqrt{1 + \langle \sigma_i^z \sigma_{i+1}^z \rangle} \left( \sqrt{1 - \langle \sigma_i^z \sigma_{i+1}^z \rangle + 2\langle \sigma_i^x \sigma_{i+1}^x \rangle} + \sqrt{1 - \langle \sigma_i^z \sigma_{i+1}^z \rangle - 2\langle \sigma_i^x \sigma_{i+1}^x \rangle} \right) & -1 < \Delta < 1, \\ 1 + \langle \sigma_i^z \sigma_{i+1}^z \rangle + \sqrt{(1 - \langle \sigma_i^z \sigma_{i+1}^z \rangle)^2 - 4\langle \sigma_i^x \sigma_{i+1}^x \rangle^2} & \text{others.} \end{cases}$$

Fig. (4) shows that the local quantum uncertainty in the region  $\Delta > 1$  decreases monotonously. There are two critical points at  $\Delta = -1$  and 1, which show the phase

transitions in both the nearest and the next to nearest neighbor spin correlations.

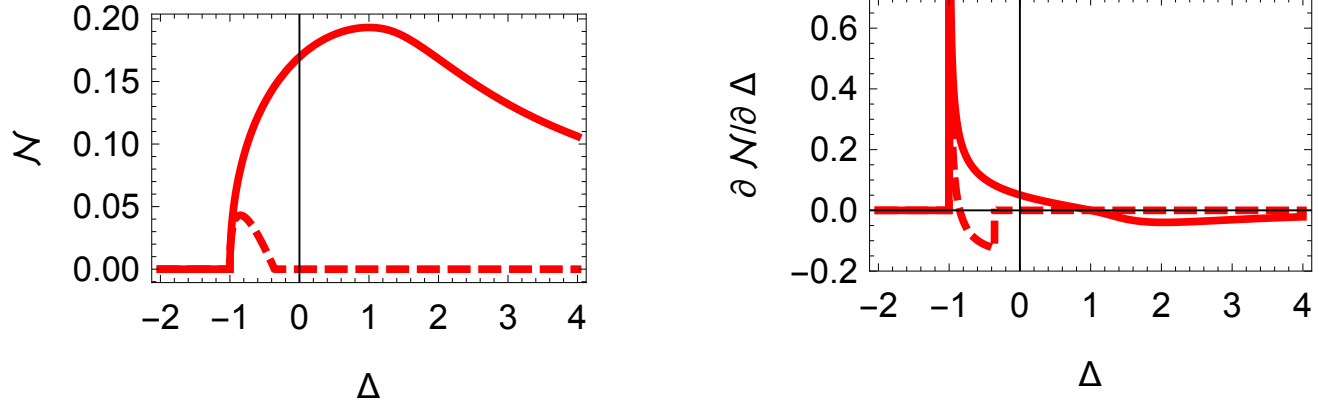


FIG. 1. (Color online) Negativity (left) and its derivative with respect to  $\Delta$  (right) vs  $\Delta$  for nearest neighbor spins (solid line) and next to nearest neighbor spins (dashed line) of the  $XXZ$  model.

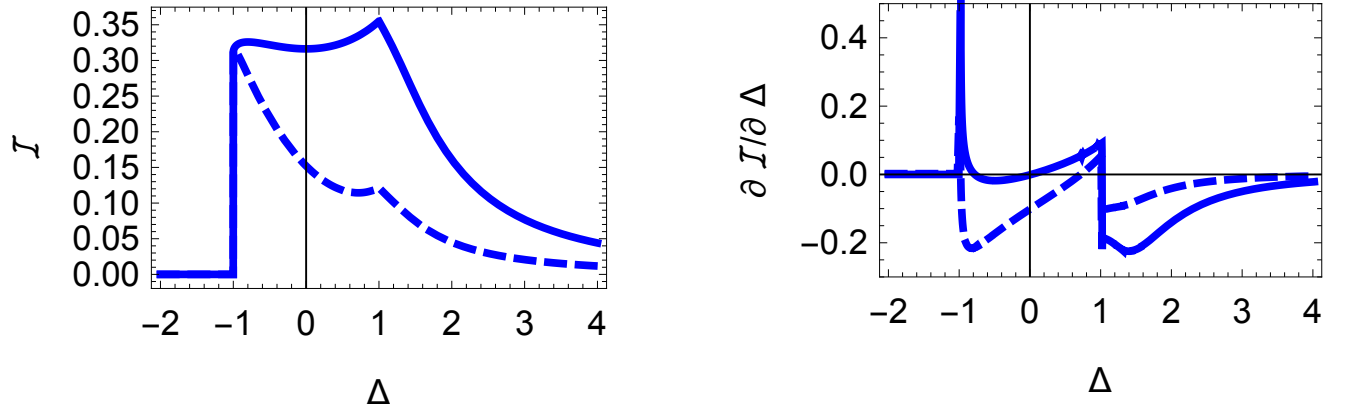


FIG. 2. (Color online) Information deficit (left) for the  $XXZ$  model for both nearest (solid line) and next to nearest (dashed line) neighbor spins and its derivative with respect to  $\Delta$  (right) vs  $\Delta$ .

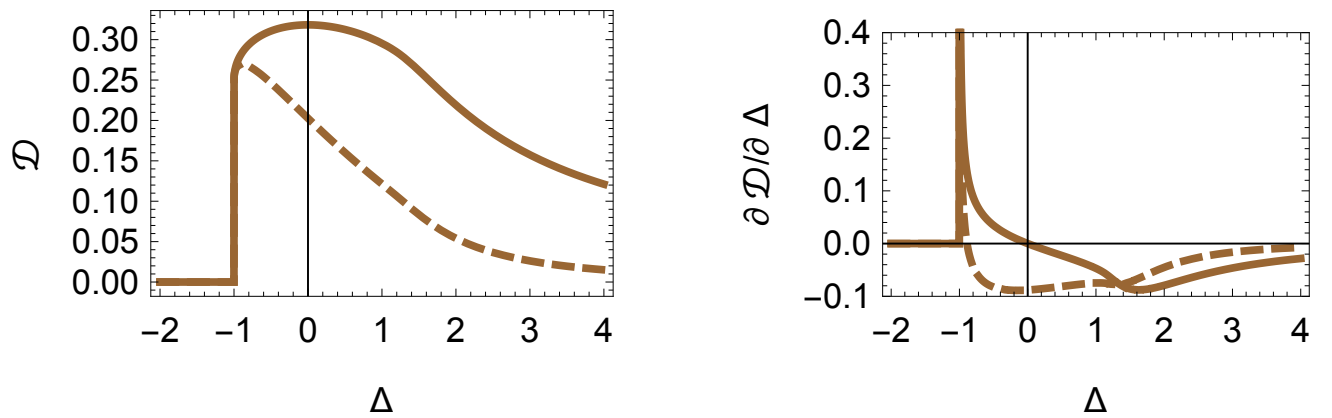


FIG. 3. (Color online) Trace distance discord (left) and its derivative with respect to  $\Delta$  (right) vs  $\Delta$  for the  $XXZ$  model for nearest (solid line) and next to nearest (dashed line) neighbor spin.

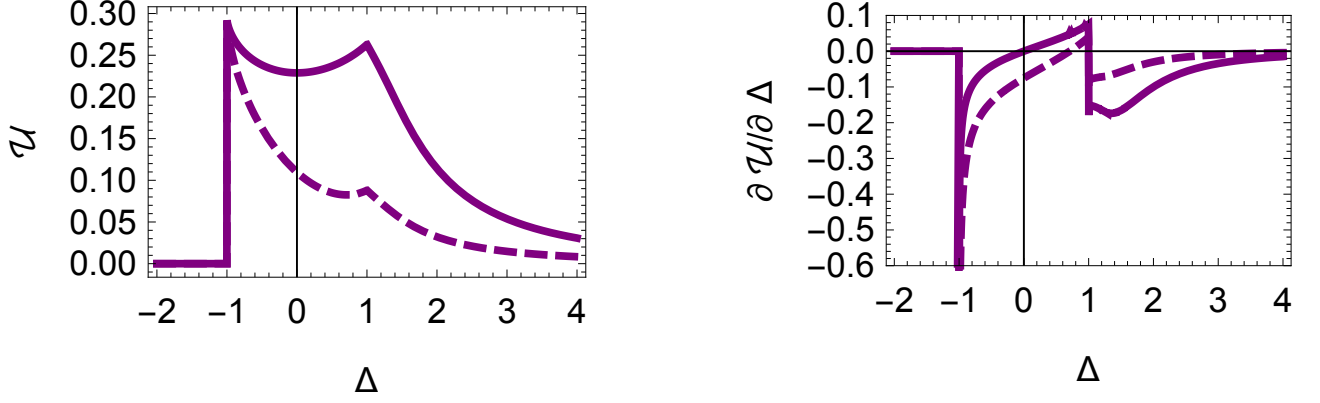


FIG. 4. (Color online) Local quantum uncertainty (left) for the  $XXZ$  model: the nearest (solid line) and the next to nearest neighbor (dashed line) spins and its derivatives (right) vs  $\Delta$ .

#### IV. LMG MODEL

We now consider the LMG model [29], which describes a two-level Fermi system  $\{|+\rangle, |-\rangle\}$ , with each level hav-

ing degeneracy  $g$ . The Hamiltonian for LMG model can be written as

$$H = \lambda \sum_{m=1}^g \frac{1}{2} (c_{+m}^\dagger c_{+m} - c_{-m}^\dagger c_{-m}) - \frac{1}{2N} \sum_{m,n=1}^g (c_{+m}^\dagger c_{-m} c_{+n}^\dagger c_{-n} + c_{-n}^\dagger c_{+n} c_{-m}^\dagger c_{+m}), \quad (22)$$

where the operators  $c_{+m}^\dagger$  and  $c_{-m}^\dagger$  create a particle in the upper and lower levels, respectively. Alternatively, the LMG model can be seen as a one-dimensional ring of spin-1/2 particles with an infinite range interaction between pairs. In fact, the Hamiltonian can be rewritten as

$$H = \lambda S_z - \frac{1}{N} (S_x^2 - S_y^2), \quad (23)$$

with  $S_z = \sum_{m=1}^N \frac{1}{2} (c_{+m}^\dagger c_{+m} - c_{-m}^\dagger c_{-m})$  and  $S_x + iS_y = \sum_{m=1}^N c_{+m}^\dagger c_{-m}$  [30]. The LMG model experiences a second-order quantum phase transitions at  $\lambda = 1$ . As  $g \rightarrow \infty$ , the ground state, as given by the HF approach, reads as

$$|HF\rangle = \prod_{m=1}^{\omega} a_{0m}^\dagger |-\rangle, \quad (24)$$

where the new levels labeled by 0 and 1 are governed by the operators

$$\begin{aligned} a_{0m}^\dagger &= \cos \alpha c_{-m}^\dagger + \sin \alpha c_{+m}^\dagger, \\ a_{1m}^\dagger &= -\sin \alpha c_{-m}^\dagger + \cos \alpha c_{+m}^\dagger. \end{aligned} \quad (25)$$

In Eq.(25),  $\alpha$  is a variational parameter to be adjusted in order to minimize energy, which is achieved according

to the choice

$$\begin{aligned} \lambda < 1 &\Rightarrow \cos 2\alpha = \lambda, \\ \lambda \geq 1 &\Rightarrow \alpha = 0. \end{aligned} \quad (26)$$

Despite being an approximation, the  $HF$  ground state provides the exact description of the critical point. The pairwise density operator for general modes  $i = (+m)$  and  $j = (-n)$  is described as

$$\rho_{i,j} = \begin{pmatrix} \langle M_i M_j \rangle & 0 & 0 & 0 \\ 0 & \langle M_i N_j \rangle & \langle c_i^\dagger c_j \rangle & 0 \\ 0 & \langle c_j^\dagger c_i \rangle & \langle N_i M_j \rangle & 0 \\ 0 & 0 & 0 & \langle N_i N_j \rangle \end{pmatrix}, \quad (27)$$

where  $M_k = 1 - N_k$  and  $N_k = c_k^\dagger c_k$ , with  $k = i, j$ . The Eq. (27) shows a  $Z_2$  symmetry.

The evaluated matrix elements of  $\rho$  for the HF ground state are given by

$$\begin{aligned} \langle M_{+m} M_{-n} \rangle &= \sin^2 \alpha \cos^2 \alpha (1 - \delta_{mn}), \\ \langle M_{+m} N_{-n} \rangle &= \cos^2 \alpha \delta_{mn} + \cos^4 \alpha (1 - \delta_{mn}), \\ \langle N_{+m} M_{-n} \rangle &= \sin^2 \alpha \delta_{mn} + \sin^4 \alpha (1 - \delta_{mn}), \\ \langle N_{+m} N_{-n} \rangle &= \sin^2 \alpha \cos^2 \alpha (1 - \delta_{mn}), \\ \langle c_{+m}^\dagger c_{-n} \rangle &= \sin \alpha \cos \alpha \delta_{mn}, \\ \langle c_{-n}^\dagger c_{+m} \rangle &= \sin \alpha \cos \alpha \delta_{mn}. \end{aligned} \quad (28)$$

Here for  $m \neq n$ , the density matrix Eq. (27) is diagonal and the state is completely pairwise uncorrelated. On the other hand, for  $m = n$ , there are quantum correlations between the modes. These correlations vanish for  $\lambda > 1$ , which gives rise to the fully polarized states.

i) Negativity of LMG. We can derive the analytical expression of negativity for the LMG model

$$\mathcal{N} = \frac{1}{2} \sqrt{1 - \lambda^2}. \quad (29)$$

ii) Information deficit for LMG. The analytical expression of information deficit for the LMG model has the following form,

$$\mathcal{I} = -\frac{\log\left(\frac{1-\lambda}{4}\right) + \log(\lambda + 1)}{2} - \lambda \tanh^{-1}(\lambda) / \ln 2. \quad (30)$$

Here, the optimal measurement is arrived at  $\theta = \phi = 0$  for Eq. (2).

iii) By tedious calculation, we have the expressions of trace distance discord for the LMG model,

$$\mathcal{D} = \frac{1}{2} \sqrt{1 - \lambda^2}, \quad (31)$$

which is the same as the measures negativity.

iv) Local quantum uncertainty for LMG. By straightforward computation, we obtain the analytical expressions of the local quantum uncertainty for LMG,

$$\mathcal{U} = 1 - \lambda. \quad (32)$$

From the above analytical results, we see that all of the four kinds of quantum correlations decrease monotonously with  $\lambda < 1$ , see Fig.(5). And in the region  $\lambda \geq 1$  the quantum correlations vanishes. One can also observe that the derivatives of the four kind quantum correlations exhibit a signature of the quantum phase transition (see the right figure in Fig. (5)).

## V. CONCLUSIONS

We have investigated the behavior of quantum correlations for the Heisenberg  $XXZ$  spin-1/2 chain via negativity, information deficit, trace distance discord and local quantum uncertainty. Some properties of the  $XXZ$  system are given as follows:

(1) Information deficit and local quantum uncertainty demonstrate the quantum phase transitions at  $\Delta = -1$  and 1. However, the negativity and trace distance discord fail to detect the quantum phase transition at  $\Delta = 1$ .

(2) For the nearest neighbor spins, entanglement and information deficit reach their maximal value at  $\Delta = 1$ . While trace distance discord has the maximal value at  $\Delta = 0$ , and local quantum uncertainty has the maximal value at  $\Delta = -1$ .

(3) The quantum correlation of the nearest neighbor spins are greater than that of the next to nearest neighbor spins for all the four kinds measures.

We have also considered quantum correlations in the Hartree-Fock ground state of the Lipkin-Meshkov-Glick model. All the four quantum correlation measures has been analytically worked out. The behaviors for both  $XXZ$  spin-1/2 chains and LMG model have been discussed. It is shown that all of the quantum correlation measures exhibit signatures of the quantum phase transitions.

We have studied the ability of quantum correlations to spotlight critical points of quantum phase transitions for an infinite spin chain described by the  $XXZ$  model, in terms of four distinct types of quantum correlations between pairs of nearest and next to nearest neighbor spins. All the measures of these quantum correlations show quantum phase transitions at  $\Delta = -1$  for both the nearest and next to nearest neighbor spins. However, the information deficit and local quantum uncertainty exhibit one more singularity at the critical point  $\Delta = 1$ . It can be seen that information deficit and local quantum uncertainty are better in studying the critical points for the  $XXZ$  spin system.

Our work highlights the type of quantum correlations involved at the quantum phase transition of the  $XXZ$  system and LMG model. These measures show the ways to explore quantum phase transition in condensed matter physics. These quantities are important tools in the investigation of quantum phase transitions in realistic experimental scenarios. The approach can be also used to explore quantum phase transitions in other physical systems.

## ACKNOWLEDGMENTS

This work is supported by the NSFC (11675113, 11765016) and Jiangxi Education Department Fund (GJJ161056, KJLD14088).

---

[1] L. Amico, R. Fazio, A. Osterloh, and V. Vedral, Rev. Mod. Phys. **80**, 517 (2008).  
 [2] R. Horodecki, P. Horodecki, M. Horodecki, and K. Horodecki, Rev. Mod. Phys. **81**, 865 (2009).  
 [3] Z. Merali, Nature **474**, 24 (2011).

[4] K. Modi, A. Brodutch, H. Cable, T. Paterek, and V. Vedral, Rev. Mod. Phys. **84**, 1655 (2012).  
 [5] G. Adesso, T. R. Bromley, and M. Cianciaruso, J. Phys. A: Math. Theor. **49**, 473001 (2016).  
 [6] H. Ollivier and W. H. Zurek, Phys. Rev. Lett. **88**, 017901 (2001).

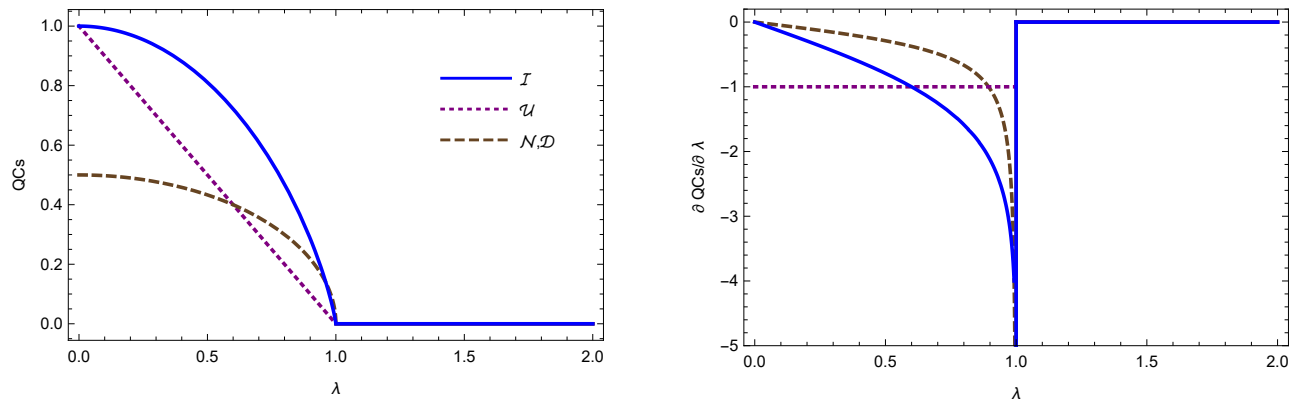


FIG. 5. (Color online) All kinds quantum correlations (QCs) and their derivative vs parameter  $\lambda$  between modes  $(+m)$  and  $(-m)$  in the HF ground state of the LMG model.

- [7] J. Oppenheim, M. Horodecki, P. Horodecki, and R. Horodecki, Phys. Rev. Lett. **89**, 180402 (2002).
- [8] B. Dakić, V. Vedral, and Č. Brukner, Phys. Rev. Lett. **105**, 190502 (2010).
- [9] F. Ciccarello, T. Tufarelli, and V. Giovannetti, New J. Phys. **16**, 013038 (2014).
- [10] D. Girolami, T. Tufarelli, and G. Adesso, Phys. Rev. Lett. **110**, 240402 (2013).
- [11] T. Werlang, C. Trippe, G. A. P. Ribeiro, and G. Rigolin, Phys. Rev. Lett. **105**, 095702 (2010).
- [12] T. Werlang, G. A. P. Ribeiro, and G. Rigolin, Phys. Rev. A **83**, 062334 (2011).
- [13] Y.-C. Li and H.-Q. Lin, Phys. Rev. A **83**, 052323 (2011).
- [14] L. Justino and T. R. de Oliveira, Phys. Rev. A **85**, 052128 (2012).
- [15] A. L. Malvezzi, G. Karpat, B. Çakmak, F. F. Fanchini, T. Debarba, and R. O. Vianna, Phys. Rev. B **93**, 184428 (2016).
- [16] M. Sarandy, Phys. Rev. A **80**, 022108 (2009).
- [17] G. Vidal and R. F. Werner, Phys. Rev. A **65**, 032314 (2002).
- [18] M. Horodecki, P. Horodecki, R. Horodecki, J. Oppenheim, A. Sen(De), U. Sen, and B. Synak-Radtke, Phys. Rev. A **71**, 062307 (2005).
- [19] A. Streltsov, H. Kampermann, and D. Bruß, Phys. Rev. Lett. **106**, 160401 (2011).
- [20] B.-L. Ye, Y.-K. Wang, and S.-M. Fei, Int. J. Theor. Phys. **55**, 2237 (2016).
- [21] E. P. Wigner and M. M. Yanase, Proc. Natl. Acad. Sci. U.S.A. **49**, 910 (1963).
- [22] S. Luo, Phys. Rev. Lett. **91**, 180403 (2003).
- [23] M. Takahashi, *Thermodynamics of one-dimensional solvable models*, Cambridge University Press (2005).
- [24] M. Shiroishi and M. Takahashi, J. Phys. Soc. Jpn. **74**, 47 (2005).
- [25] M. Takahashi, G. Kato, and M. Shiroishi, J. Phys. Soc. Jpn. **73**, 245 (2004).
- [26] G. Kato, M. Shiroishi, M. Takahashi, and K. Sakai, J. Phys. A: Math. Gen. **37**, 5097 (2004).
- [27] G. Kato, M. Shiroishi, M. Takahashi, and K. Sakai, J. Phys. A: Math. Gen. **36**, L337 (2003).
- [28] R. Dillenschneider, Phys. Rev. B **78**, 224413 (2008).
- [29] H. J. Lipkin, N. Meshkov, and A. J. Glick, Nucl. Phys. **62**, 188 (1965).
- [30] P. Ring and P. Schuck, *The nuclear many-body problem*, Springer Science & Business Media (2004).